

# THE COMPARISON OF THE EXPRESSIONS FOR DTR ANGULAR DENSITY IN LAUE AND BRAGG SCATTERING GEOMETRIES

*S.V. Blazhevich, R.A. Zagorodnyuk, A.V. Noskov*  
*Belgorod National Research University, Belgorod, Russia*  
*E-mail: noskovbupk@mail.ru*

In the present work, the expressions for angular density of DTR generated in a single-crystal target by a relativistic electron are derived for cases of Laue and Bragg scattering geometries. The derived expressions have been compared. The following two extremal cases have been considered when the path of the electron in the target is much longer or much shorter than the extinction length of X-ray waves in the single crystal.

PACS: 41.60.-m; 41.75.Ht; 42.25.Fx

## INTRODUCTION

The knowledge of spatial and angular distributions of particles in the incident beam is important for the experimental data interpretation in the physics of interaction of relativistic electrons with matter. That is why the working out of express methods of obtaining information about the characteristics of the beam used in the experiment is actual problem. One of the approaches is to use different types of radiation excited by relativistic charged particles in matter. Recently the possibility of use of parametric X-radiation (PXR) for the diagnostics of relativistic electron beams was experimentally studied in [1, 2]. In [3] it was suggested using PXR generated in a thin crystal to get operative information on spatial distribution of the relativistic electron beam. The applicability of transition radiation (TR) of vacuum ultraviolet range to measure the electron beam cross dimensions was demonstrated in [4].

When a charged particle crosses the crystal plate surface, the transition radiation (TR) takes place [5]. TR appearing on the border diffracts then on a system of parallel atomic planes of the crystal which forms DTR in a narrow spectral range [6 - 9]. The DTR photons move near the Bragg scattering direction. In the work [10], the expression describing DTR was obtained in dynamical approach for a special case of symmetrical reflection of relativistic electron Coulomb field relative to the target surface in the Bragg scattering geometry. In [10] there was shown a good agreement of theory with experiment. In the recent work [11] the expression describing DTR in the Bragg scattering geometry was obtained in kinematical approach for the symmetric reflection case.

The process of coherent X-ray radiation by a single relativistic electron in a crystal is described in the framework of the dynamical theory of x-rays diffraction in [12 - 15]. In these papers, the dynamic theory of coherent X-ray radiation generated by a relativistic electron in a crystal are built for general case of asymmetric relative to the crystal (target) surface reflection of the electron Coulomb field. In this case, the system of the parallel reflecting atomic planes in the target can be located at arbitrarily given angle to the target surface. For divergent beam of relativistic electrons, the dynamic theory was developed in the resent works both in Laue scattering geometry [16] and in Bragg scattering geometry [17, 18].

In the present work DTR of a relativistic electron in the electron beam crossing a monocrystalline target

have been considered both in Laue and Bragg scattering geometries. The expressions for angular density of the radiation are derived. The obtained expressions have been compared in interesting cases when the path of the relativistic electron is much less or much more than the extinction length of x-ray waves in the monocrystalline target.

## THE RADIATION PROCESSES GEOMETRIES

Let us consider a beam of relativistic electrons crossing a monocrystalline plate in Laue (Fig. 1) and Bragg (Fig. 2) scattering geometries.

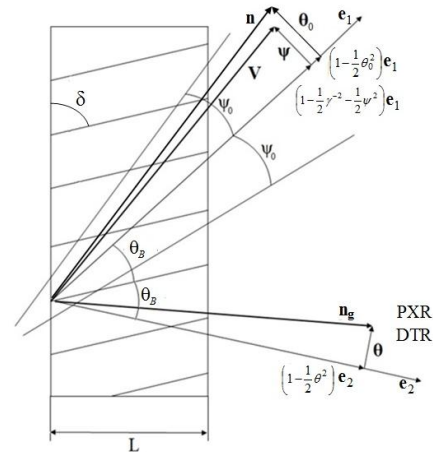


Fig. 1. Laue scattering geometry

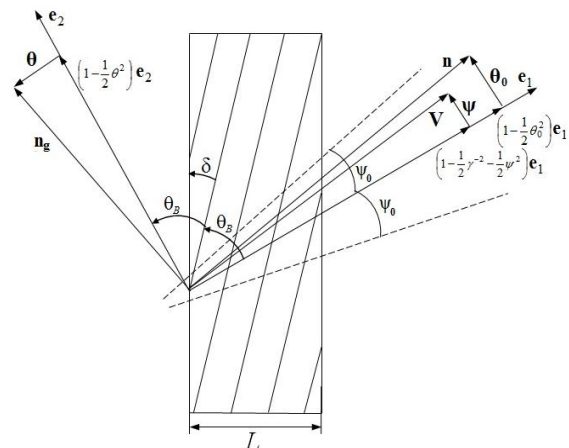


Fig. 2. Bragg scattering geometry

Let us involve the angular variables  $\psi$ ,  $\theta$  and  $\theta_0$  in accordance with the definition of relativistic electron velocity  $\mathbf{V}$  and unit vectors in direction of momentum

of the photon radiated in the direction near electron velocity vector  $\mathbf{n}$  and in the of Bragg scattering direction  $\mathbf{n}_g$ :

$$\begin{aligned}\mathbf{V} &= \left(1 - \frac{1}{2}\gamma^{-2} - \frac{1}{2}\psi^2\right)\mathbf{e}_1 + \boldsymbol{\psi}, \\ \mathbf{e}_1\boldsymbol{\psi} &= 0, \quad \mathbf{n} = \left(1 - \frac{1}{2}\theta_0^2\right)\mathbf{e}_1 + \boldsymbol{\theta}_0, \\ \mathbf{e}_1\boldsymbol{\theta}_0 &= 0, \quad \mathbf{e}_1\mathbf{e}_2 = \cos 2\theta_B, \\ \mathbf{n}_g &= \left(1 - \frac{1}{2}\theta^2\right)\mathbf{e}_2 + \boldsymbol{\theta}, \quad \mathbf{e}_2\boldsymbol{\theta} = 0,\end{aligned}\quad (1)$$

where  $\boldsymbol{\theta}$  is the radiation angle, counted from direction of axis of radiation detector  $\mathbf{e}_2$ ,  $\boldsymbol{\psi}$  is the incidence angle of an electron in the beam counted from the electron beam axis  $\mathbf{e}_1$ ,  $\boldsymbol{\theta}_0$  is the angle between the movement direction of incident photon and axis  $\mathbf{e}_1$ ,  $\gamma = 1/\sqrt{1-V^2}$  is Lorentz-factor of the particle. The angular variables are decomposed into the components parallel and perpendicular to the figure plane:  $\boldsymbol{\theta} = \boldsymbol{\theta}_{\parallel} + \boldsymbol{\theta}_{\perp}$ ,  $\boldsymbol{\theta}_0 = \boldsymbol{\theta}_{0\parallel} + \boldsymbol{\theta}_{0\perp}$ ,  $\boldsymbol{\psi} = \boldsymbol{\psi}_{\parallel} + \boldsymbol{\psi}_{\perp}$ .  $\psi_0$  is

$$\left(\frac{dN_{\text{DTR}}^{(s)}}{d\Omega}\right)_L = \frac{e^2|\chi'_g|C^{(s)2}}{2\pi^2\sin^2\theta_B} \Sigma^{(s)2} \int_{-\infty}^{\infty} \frac{\varepsilon^2}{\xi^{(s)2} + \varepsilon} \sin^2\left(b_L^{(s)} \frac{\sqrt{\xi^{(s)2} + \varepsilon}}{\varepsilon}\right) d\xi^{(s)}(\omega), \quad (3)$$

where

$$\begin{aligned}\Sigma^{(s)} &= \Omega^{(s)} \left( \frac{1}{\gamma^{-2} + (\theta_{\perp} - \psi_{\perp})^2 + (\theta_{\parallel} + \psi_{\parallel})^2} - \frac{1}{\gamma^{-2} + (\theta_{\perp} - \psi_{\perp})^2 + (\theta_{\parallel} + \psi_{\parallel})^2 - \chi_0'} \right), \\ \Omega^{(1)} &= \theta_{\perp} - \psi_{\perp}, \quad \Omega^{(2)} = \theta_{\parallel} + \psi_{\parallel}, \quad \varepsilon = \frac{\sin(\delta + \theta_B)}{\sin(\delta - \theta_B)}, \quad b_L^{(s)} = \frac{1}{2\sin(\delta - \theta_B)} \frac{L}{L_{\text{ext}}}, \\ \xi^{(s)}(\omega) &= \eta^{(s)}(\omega) + \frac{1-\varepsilon}{2\nu^{(s)}}, \quad L_{\text{ext}}^{(s)} = 1/\omega|\chi'_g|C^{(s)}, \quad \eta^{(s)}(\omega) = \frac{2\sin^2\theta_B}{V^2|\chi'_g|C^{(s)}} \left(1 - \frac{\omega(1 - \theta_{\parallel}\cot\theta_B)}{\omega_B}\right),\end{aligned}\quad (4)$$

$$\nu^{(s)} = \frac{\chi'_g C^{(s)}}{\chi_0'}, \quad \omega_B = gV/2\sin\theta_B \text{ is the Bragg frequency, } \theta_B \text{ is the Bragg angle.}$$

The parameter  $\varepsilon$  is an important parameter in (3); it determines the degree of asymmetry of the reflection of the field in a crystal plate with respect to the target surface. Note that the angle of electron incidence on the target surface  $\delta - \theta_B$  increases when the  $\varepsilon$  parameter decreases, and vice versa.

Parameter  $b_L^{(s)}$  characterizing the thickness of the crystal plate is the ratio of half of the path of the electron in the target  $L_e = L/\sin(\delta - \theta_B)$  to the extinction length  $L_{\text{ext}}^{(s)}$ . Parameter  $\nu^{(s)}$  can take the values in the interval  $0 \leq \nu^{(s)} \leq 1$  and determines the degree of re-

$$\left(\frac{dN_{\text{DTR}}^{(s)}}{d\Omega}\right)_B = \frac{e^2|\chi'_g|C^{(s)2}}{2\pi^2\sin^2\theta_B} \Sigma^{(s)2} \int_{-\infty}^{\infty} \frac{\varepsilon^2}{\xi^{(s)2} - (\xi^{(s)2} - \varepsilon)\coth^2\left(\frac{b_B^{(s)}\sqrt{\varepsilon - \xi^{(s)2}}}{\varepsilon}\right)} d\xi^{(s)}(\omega), \quad (5)$$

the divergence parameter of the beam of radiating electrons.

Let us consider electromagnetic processes in the crystalline medium characterized by complex permittivity

$$\varepsilon(\omega, \mathbf{r}) = 1 + \chi(\omega, \mathbf{r}), \quad (2)$$

where

$$\chi(\omega, \mathbf{r}) = \chi_0(\omega) + \sum_{\mathbf{g}}' \chi_{\mathbf{g}}(\omega) \exp(i\mathbf{g}\mathbf{r}), \quad \chi(\omega, \mathbf{r}) \text{ is}$$

the dielectric susceptibility,  $\chi_{\mathbf{g}}(\omega) = \chi_{\mathbf{g}}'(\omega) + i\chi_{\mathbf{g}}''(\omega)$  is the Fourier coefficient of the expansion of the dielectric susceptibility of the crystal in reciprocal lattice vectors  $\mathbf{g}$ , and  $\chi_0(\omega)$  is the average dielectric susceptibility.

### ANGULAR DENSITY DTR IN A THIN CRYSTAL

Let us write the expression describing the angular densities of DTR generated by relativistic electron crossing a single crystal plate in Laue scattering geometry [18]:

flection of the waves from the crystal, which is caused by the nature of the interference of the waves reflected from different planes (constructive ( $\nu^{(s)} \approx 1$ ) or destructive ( $\nu^{(s)} \approx 0$ ). The spectral function  $\eta^{(s)}(\omega)$  rapidly changes with the frequency of the radiation therefore this function is convenient for use as an argument in the diagrams demonstrating the spectra of PXR and DTR.

The expression describing the angular densities of DTR in Bragg scattering geometry derived in [16] has the view

$$C^{(2)} = |\cos 2\theta_B|, \quad \varepsilon = \frac{\sin(\theta_B - \delta)}{\sin(\theta_B + \delta)}, \quad b_B^{(s)} = \frac{1}{2\sin(\theta_B + \delta)} \frac{L}{L_{ext}^{(s)}}, \quad \xi^{(s)}(\omega) = \eta^{(s)}(\omega) + \frac{1 + \varepsilon}{2\nu^{(s)}}. \quad (6)$$

Under a fixed value of  $\theta_B$  the value  $\varepsilon$  (6) defines the orientation of the crystal plate surface in relation to the system of diffracting atomic planes. When the angle of electron incidence on the target surface  $\theta_B + \delta$  decreases the value of  $\delta$  parameter can become negative and then will increase in magnitude (in extreme case  $\delta \rightarrow -\theta_B$ ) that leads to increase in  $\varepsilon$ . On the contrary, when the angle of electron incidence decreases the value of  $\varepsilon$  decreases (in extreme case  $\delta \rightarrow \theta_B$ ).

Let us consider the extreme case when the electron path in the target expressed in extinction length is  $b^{(s)} \ll \sqrt{\varepsilon}$  or  $b^{(s)} \gg \sqrt{\varepsilon}$ . Let us write these inequalities in view  $\frac{L_e}{L_{ext}^{(s)}} \ll 2\sqrt{\varepsilon}$ ,  $\frac{L_e}{L_{ext}^{(s)}} \gg 2\sqrt{\varepsilon}$ . Because the parameter  $\varepsilon$  in the real experiments possesses the value  $0.5 < \varepsilon < 3$  the pointed inequalities practically correspond to inequalities  $L_e \ll L_{ext}^{(s)}$ ,  $L_e \gg L_{ext}^{(s)}$ .

The extreme approximations of integrals of DTR spectra for Laue and Bragg scattering geometries we will obtain in following view

$$\int_{-\infty}^{\infty} \frac{\varepsilon^2}{\xi^{(s)2} + \varepsilon} \sin^2 \left( b_L^{(s)} \frac{\sqrt{\xi^{(s)2} + \varepsilon}}{\varepsilon} \right) d\xi^{(s)}(\omega) \approx \quad (7)$$

$$\approx \begin{cases} \frac{\varepsilon\sqrt{\varepsilon}\pi}{2}, & b_L^{(s)} \gg \sqrt{\varepsilon} \\ \pi\varepsilon b_L^{(s)}, & b_L^{(s)} \ll \sqrt{\varepsilon}, \end{cases}$$

$$\int_{-\infty}^{\infty} \frac{\varepsilon^2}{\xi^{(s)2} - (\xi^{(s)2} - \varepsilon) \coth^2 \left( \frac{b_B^{(s)} \sqrt{\varepsilon - \xi^{(s)2}}}{\varepsilon} \right)} d\xi^{(s)}(\omega) = \quad (8)$$

$$= \varepsilon\sqrt{\varepsilon}\pi \cdot \tanh \left( \frac{b_B^{(s)}}{\sqrt{\varepsilon}} \right) \approx \begin{cases} \varepsilon\sqrt{\varepsilon}\pi, & b_B^{(s)} \gg \sqrt{\varepsilon} \\ \pi\varepsilon b_B^{(s)}, & b_B^{(s)} \ll \sqrt{\varepsilon}. \end{cases}$$

The approximations (7) were obtained in [18].

Using the obtained approximations, we will derive the angular densities of DTR in Laue and Bragg scattering geometries for conditions  $b_L^{(s)} \ll \sqrt{\varepsilon}$  and  $b_B^{(s)} \ll \sqrt{\varepsilon}$  correspondently

$$\left( \frac{dN_{DTR}^{(s)}}{d\Omega} \right)_L \stackrel{b_L^{(s)} \ll \sqrt{\varepsilon}}{=} \frac{e^2 \omega_B \chi_g'^2 C^{(s)2}}{4\pi \sin^2 \theta_B} \Sigma^{(s)2} \varepsilon \frac{L}{\sin(\delta - \theta_B)} \quad (9)$$

and

$$\left( \frac{dN_{DTR}^{(s)}}{d\Omega} \right)_B \stackrel{b_B^{(s)} \ll \sqrt{\varepsilon}}{=} \frac{e^2 \omega_B \chi_g'^2 C^{(s)2}}{4\pi \sin^2 \theta_B} \Sigma^{(s)2} \varepsilon \frac{L}{\sin(\theta_B + \delta)}. \quad (10)$$

In the cases when  $b_L^{(s)} \gg \sqrt{\varepsilon}$  and  $b_B^{(s)} \gg \sqrt{\varepsilon}$  the expressions (3) and (5) will take the view

$$\left( \frac{dN_{DTR}^{(s)}}{d\Omega} \right)_L \stackrel{b_L^{(s)} \gg \sqrt{\varepsilon}}{=} \frac{e^2 \omega_B \chi_g'^2 C^{(s)2}}{4\pi \sin^2 \theta_B} \Sigma^{(s)2} \varepsilon \sqrt{\varepsilon}, \quad (11)$$

$$\left( \frac{dN_{DTR}^{(s)}}{d\Omega} \right)_B \stackrel{b_B^{(s)} \gg \sqrt{\varepsilon}}{=} \frac{e^2 \omega_B \chi_g'^2 C^{(s)2}}{2\pi \sin^2 \theta_B} \Sigma^{(s)2} \varepsilon \sqrt{\varepsilon}. \quad (12)$$

The expressions (9) and (10) describing the angular densities of DTR in Laue and Bragg geometries are coincided in the case of  $b^{(s)} \ll \sqrt{\varepsilon}$ . Let us note that the condition  $b^{(s)} \ll \sqrt{\varepsilon}$  means the length of electron path in the target is considerably less than the extinction length of x-ray waves in the crystal  $L_e \ll L_{ext}^{(s)}$  that completely excludes repumping incident and diffracted waves in each other.

If the electron path much more than extinction length of x-ray waves in target  $b^{(s)} \gg \sqrt{\varepsilon}$  ( $L_e \gg L_{ext}^{(s)}$ ) then the DTR angular density in Bragg scattering geometry (12) exactly two times exceeds the density in Laue geometry (11).

## CONCLUSIONS

In the present work, the expressions for angular density of DTR generated by relativistic electron in a thin nonabsorbing target in Laue and Bragg scattering geometries have been derived. The expressions have been derived also for conditions when the electron path in the target is much less than extinction length of x-ray waves in the target. It has been shown that in this case the expressions for DTR angular density in Laue and Bragg geometry are almost coincided.

The expressions have been derived also for conditions when the electron path in the target is much more than extinction length of x-ray waves in the target. It has been shown that in this case the DTR angular density in Bragg scattering geometry exactly two times exceeds the density in Laue geometry.

## ACKNOWLEDGEMENTS

This work was supported by the Ministry of Education and Science of the Russian Federation (state task № 3.4877.2017/BY).

## REFERENCES

1. Y. Takabayashi. Parametric X-ray radiation as a beam size monitor // *Phys. Lett. A.* 2012, v. 376, p. 2408.
2. Y. Takabayashi, K. Sumitani. New method for measuring beam profiles using a parametric X-ray pinhole camera // *Phys. Lett. A.* 2013, v. 377, p. 2577.
3. A. Gogolev, A. Potylitsyn, G. Kube. A possibility of transverse beam size diagnostics using parametric X-ray radiation // *J. Phys. Conference Series.* 2012, v. 357, 012018.
4. L.G. Sukhikh, S.Yu. Gogolev, A.P. Potylitsyn. Backward transition radiation in EUV-region as a possible tool for beam diagnostics // *J. Phys. Conference Series.* 2010, v. 236, 012011.

5. V.L. Ginzburg, V.N. Tsytovich. *Transition Radiation and Transition Scattering*. M.: "Nauka", 1984.
6. A. Caticha. Transition-diffracted radiation and the Čerenkov emission of x-rays // *Phys. Rev. A*. 1989, v. 40, p. 4322.
7. V. G. Baryhevsky. Parametric X-ray radiation at a small angle near the velocity direction of the relativistic particle // *Nucl. Instr. and Meth. A*. 1997, v. 122, p. 13.
8. X. Artru, P. Rullhusen. Parametric X-rays and diffracted transition radiation in perfect and mosaic crystals // *Nucl. Instr. and Meth. B*. 1998, v. 145, p. 1.
9. N. Nasonov. Influence of the density effect upon the parametric X-rays of high energy particles // *Phys. Lett. A*. 1998, v. 246, p. 148.
10. Y.N. Adishev, S.N. Arishev, A.V. Vnukov, A.V. Vukolov, A.P. Potylitsyn, S.I. Kuznetsov, V.N. Zabaev, B.N. Kalinin, V.V. Kaplin, S.R. Uglov, and A.S. Kubankin. Angular distribution of X-ray radiation by 500 MeV electrons in a tungsten crystal // *Nucl. Instr. and Meth. B*. 2003, v. 201(1), p. 114.
11. I. Chaikovska, R. Chehab, X. Artru, A.V. Shchagin. Characteristic, parametric, and diffracted transition X-ray radiation for observation of accelerated particle beam profile // *Nucl. Instr. and Meth. B*. 2017, v. 402, p. 75.
12. S.V. Blazhevich, A.V. Noskov. On the dynamical effects in the characteristics of transition radiation produced by a relativistic electron in a single crystal plate // *Nucl. Instr. and Meth. B*. 2006, v. 252, p. 69.
13. S.V. Blazhevich, A.V. Noskov. Coherent X-radiation of relativistic electron in a single crystal under asymmetric reflection conditions // *Nucl. Instr. and Meth. B*. 2008, v. 266, p. 3770.
14. S. Blazhevich, A. Noskov. Parametric X-ray radiation along relativistic electron velocity in asymmetric Laue geometry // *J. Exp. Theor. Phys.* 2009, v. 109, p. 901.
15. S.V. Blazhevich, A.V. Noskov. Coherent X-Ray Radiation Excited by a Diverging Relativistic Electron Beam in a Single Crystal // *J. Exp. Theor. Phys.* 2015, v. 120, p. 753.
16. S.V. Blazhevich, Yu.A. Boltenko, T.V. Koskova, A.A. Mazilov, A.V. Noskov. Influence of relativistic electron beam divergence on angular characteristics of PXR and DTR generated in a single-crystal plate in Bragg scattering geometry // *Problems of Atomic Science and Technology. Series "Physics of Radiation Effect and Radiation Materials Science"*. 2015, № 5(99), p. 3.
17. S.V. Blazhevich, I.V. Kolosova, N.A. Koren'kova, A.A. Mazilov, A.V. Noskov. Influence of multiple scattering on dynamical effect manifestation in coherent X-ray radiation by relativistic electron // *Problems of Atomic Science and Technology. Series "Nuclear Physics Investigations"*. 2016, № 3(103), p. 87.
18. S.V. Blazhevich, A.V. Noskov. Diffracted Transition Radiation of an Ultra-High-Energy Relativistic Electron Beam in a Thin Single-Crystal Wafer // *J. Exp. Theor. Phys.* 2016, v. 123, p. 901.

*Article received 25.09.2017*

### СРАВНЕНИЕ ВЫРАЖЕНИЙ ДЛЯ УГЛОВОЙ ПЛОТНОСТИ ДПИ В ГЕОМЕТРИЯХ РАССЕЯНИЯ ЛАУЭ И БРЭГГА

*С.В. Блажевич, Р.А. Загороднюк, А.В. Носков*

Выражения для угловой плотности ДПИ, генерируемого в монокристаллической мишени релятивистским электроном, выведены для случая геометрии рассеяния Лауэ и Брэгга. Проведено сравнение полученных выражений. Рассмотрены два экстремальных случая, когда путь электрона в мишени много больше или много меньше длины экстинкции рентгеновских волн в монокристалле.

### ПОРІВНЯННЯ ВИРАЗІВ ДЛЯ КУТОВОЇ ЩІЛЬНОСТІ ДПВ В ГЕОМЕТРІЇ РОЗСІЯННЯ ЛАУЕ І БРЕГА

*С.В. Блажевич, Р.А. Загороднюк, А.В. Носков*

Виразення для кутової щільності ДПВ, генерованого в монокристалічній мішені релятивістським електроном, виведені для випадку геометрії розсіяння Лауе і Брега. Проведено порівняння отриманих виразів. Розглянуто два екстремальні випадки, коли шлях електрона в мішені багато більше або багато менше довжини екстинкції рентгенівських хвиль у монокристалі.